Effects of image lag on real-time target tracking in radiotherapy

doi: 10.1117/12.844202

Effects of image lag on real-time target tracking in radiotherapy

R. Tanaka*[a], K. Ichikawa[a], S. Mori [b], S. Dobashi [b],
M. Kumagaya [b], H. Kawashima[a], S. Morita [b], S. Sanada[a]
[a] Dep. of Radiological Technology, School of Health Sciences, College of Medical, Pharmaceutical and Health Sciences, Kanazawa University; 5-11-80 Kodatsuno, Kanazawa, Japan 920-0942
[b] Research Center for Charged Particle Therapy, National Institute of Radiological Sciences; 4-9-1 Anagawa, Inage-ku, Chiba, Japan 263-8555

ABSTRACT

There is a concern that image lag may reduce accuracy of real-time target tracking in radiotherapy. This study was performed to investigate influence of image lag on the accuracy of target tracking in radiotherapy. Fluoroscopic images were obtained using a direct type of dynamic flat-panel detector (FPD) system under conditions of target tracking during radiotherapy. The images continued to be read out after X-irradiations and cutoff, and image lag properties in the system were then determined. Subsequently, a tungsten materials plate with a precision edge was mounted on to a motor control device, which provided a constant velocity. The plate was moved into the center of the detector at movement rate of 10 and 20 mm/s, covering lung tumor movement of normal breathing, and MTF and profile curves were measured on the edges covering and uncovering the detector. A lung tumor with blurred edge due to image lag was simulated using the results and then superimposed on breathing chest radiographs of a patient. The moving target with and without image lag was traced using a template-matching technique. In the results, the target could be traced within a margin for error in external radiotherapy. The results indicated that there was no effect of image lag on target tracking in usual breathing speed in a radiotherapy situation. Further studies are required to investigate influence by the other factors, such as exposure dose, target size and shape, imaging rate, and thickness of a patient's body.

Keywords: Image lag, flat panel detector, radiotherapy, target tracking

1. INTRODUCTION

Real-time tumor tracking in external radiotherapy can be achieved by diagnostic (kilovoltage) X-ray imaging with a dynamic flat-panel detector (FPD).[1-3] These FPD systems are expected to solve the problems of low image contrast and quality seen in megavoltage imaging. Accuracy of target tracking is directly linked to treatment results, and therefore image qualitiy is a major concern, especially with regard to image lag and ghosting, which may induce blurring on the contours of a moving target. Lag is the carryover of image charge generated by previous X-ray exposures into subsequent image frames. Ghosting is the change of X-ray sensitivity, or gain, of the detector as a result of previous radiation exposure. Lag and ghosting in a-Se FPDs are determined by the properties of both the a-Se layer and the active matrix.[4,5] Previous studies indicated that primary a-Se FPDs showed a lag in the first frame after X-ray exposure of less than 5%.[6-9] Modifications in the technology of the a-Se detectors appear to have resulted in marked decreases in both lag and ghosting effects in more recent systems.[10-12] Recently, several methods for measuring temporal modulation transfer function (MTF) and detective quantum efficiency (DQE) have been proposed and the properties of FPDs used in dynamic imaging have been reported.[13-15] However, there have been no studies regarding how image lag and ghosting affect motion tracking by dynamic imaging with FPDs. In external radiotherapy, there is concern regarding the relationship between image quality and total patient dose during real-time tumor tracking, because it is necessary to optimize imaging parameters in each patient to keep patient dose as low as possible while maintaining tracking accuracy. Our ultimate goal is to develop a simulation system to determine appropriate imaging parameters in consideration of total patient dose and image quality, such as MTF, DQE, and image lag. Here, we investigated image lag properties during target tracking in external radiotherapy. The purpose of this study was to address image lag properties in target tracking and its influence on the accuracy of tumor tracking.

*rie44@mhs.mp.kanazawa-u.ac.jp; phone 81 76 265-2537; fax 81 76 234-4366;

Medical Imaging 2010: Physics of Medical Imaging, edited by Ehsan Samei, Norbert J. Pelc,
Proc. of SPIE Vol. 7622, 76224S · © 2010 SPIE · CCC code: 1605-7422/10/$18 · doi: 10.1117/12.844202

2. MATERIALS AND METHODS

Imaging devices and geometry

Dynamic images were obtained using a dynamic FPD system (SONIALVISION Safire2; Shimadzu, Kyoto, Japan). Two sets of FPD and X-ray tubes with the same performance were mounted at a 90° angle in our system (Fig. 1). The X-ray tubes were set opposite the positions of each FPD and the source-to-image distance (SID) was 1.0 m. The FPD was a direct type consisting of an a-Se/TFT imaging array and the maximum imaging rate was 30 frames per second (fps). In this study, one of the FPDs was examined. The experiments were performed according to IEC 62220-1 standard except SID.[16] The matrix size was 1024×1024 pixels, the pixel size was 248×248 μm, field of view was 25.4×25.4 cm, and the grayscale range of the images was 16 bits, which was proportional to the incident exposure in the FPD.

Lag measurement

Lag measurement experiments were performed at a standard X-ray spectrum without grid (IEC RQA5; 70 kV, 23 mA, 4 ms, 3.2 mR). After irradiation more than 10 times, the X-ray was cutoff and images continued to be read out and stored. IEC 62220-1-3 standard shows two requirements in the number of stored images; one is a power of 2 and the other is stable mean pixel value in the obtained images, and recommends acquisition of 64 images.[17] However, in the present study, 32 images were stored due to system limitations. Note that the image sets were confirmed to fulfill the requirements, *i.e.*, stability of mean pixel values. The region of interest (ROI) measuring 256×256 pixels was located manually on the detector center and average pixel value was measured using Image-J ver. 1.42 (http://rsb.info.nih.gov/ij/) (Fig. 2). Image lag can be defined as the carryover of trapped charge generated by X-ray exposure into subsequent image frames acquired with no X-ray exposure, and that in the *n*th frame (L_n) can be calculated as follows[4]:

$$L_n = \left(\frac{S_n - B}{S_0 - B} \right) \times 100 \tag{1}$$

where S_n and S_0 are the average pixel values measured in ROI in frame number n and the 0th frame acquired immediately following X-irradiation and cutoff, respectively. The term B is the pixel value measured in the background image, which was obtained without any radiation. Three sets of images were evaluated and the average L_n value was calculated in each *n*th frame from X-ray cutoff.

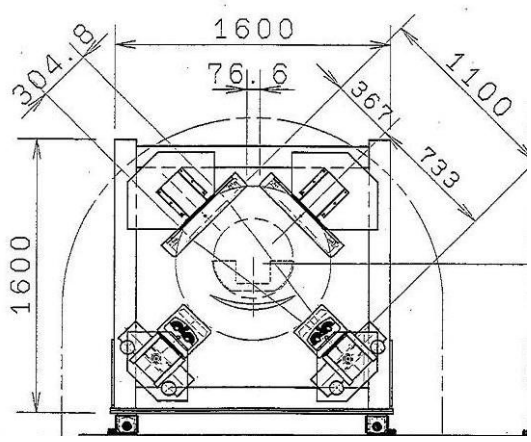

Figure 1. Geometry of the FPD system evaluated in this study. The system was developed for real-time target tracking in three dimensions for external radiotherapy. Source-to-target distance was limited to 1.0 m.

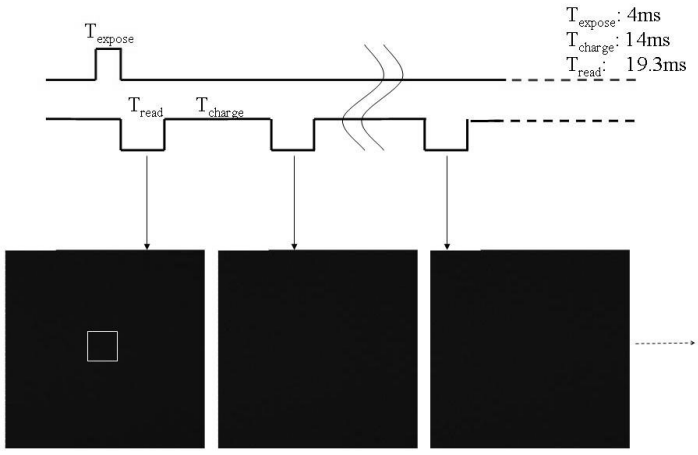

Figure 2. Imaging chart and images obtained. Images were read after exposure. The white square shows the region of interest (ROI) for measuring pixel values to determine image lag.

MTF measurement

A tungsten materials plate with a precision edge (thickness, 1 mm; size, 10 × 10 cm; IEC standard) was mounted onto a motor control device, which provided a constant velocity. The plate was positioned in such a way that the edge was slightly (~2°) tilted with respect to the axis of the image matrix. The plate was moved into the center of the detector in contact with the detector surface. Figure 3 shows imaging chart and images of a tungsten materials plate. The movement rate was 10 and 20 mm/s, covering lung tumor movement of normal breathing. Imaging was performed under conditions of target tracking in external radiotherapy (15 fps, 70 kV, 23 mA, 4 ms). Images of the static plate were also obtained for comparison between the results in dynamic and static states. Profile curves of average pixel values in 50 rows were obtained in both edges covering and uncovering the detector, to evaluate image blurring visually and quantitatively. Subsequently, ROIs of 256×256 pixels were located on the edges covering and uncovering the detector. The frame with the edge closest to the detector center was used to calculate the MTF. Measurements obtained by covering the detector were referred to as the "falling edge," and those obtained by uncovering the detector were referred to as the "rising edge." For determination of MTF, the method given in the IEC standard was used.[16] The standard process of derivation of the edge spread function (ESF) to obtain the line spread function (LSF) and subsequent fast Fourier transform to obtain the presampled MTF was applied.

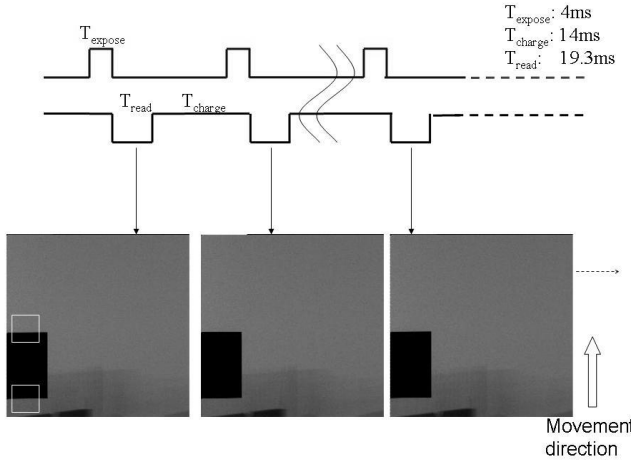

Figure 3. Imaging chart and images of a moving tungsten materials plate (70kV, 1.4mAs, 15fps, attached Al filter 4mm). The white square shows the region of interest (ROI) to measure MTF.

Creation of simulated images

A digital phantom of the lung nodule was used as a target in this study. The phantom was created based on Gaussian distribution as follows:

$$f(x) = \frac{1}{\sqrt{2\pi}\sigma}\exp\left(-\frac{(x-\mu)^2}{2\sigma^2}\right) \quad (0 \le x < \mathrm{X}) \tag{2}$$

where x is the distance from the center of the Gaussian distribution, μ is displacement from the center, and σ is standard divisions. In this study, X and σ were 120 and 25 pixels, respectively, to create a round target visually 1 cm in diameter, and μ was determined by multiplying the frame number going back from $n = 0$ and a movement rate in units of pixels/frame. The targets moving at rates of 10 mm/s and 20 mm/s were displaced by 2.7 and 5.4 pixels/frame, respectively. The target in the nth frame $T(n)$ is described as:

$$T(n) = P \times f(x), \tag{3}$$

where P is the pixel value at the center of the target, which was determined based on the pixel value of soft tissues around the insert position. A moving target in the nth frame $T_{lag}(n)$ was simulated using the results of "2.2. Lag measurement" as follows:

$$T_{lag}(n) = T(n) + \sum_{k=1}^{K}\{T(n-k) \times L_k\} \tag{4}$$

where k is the frame number going back from the n^{th} frame of interest, and L_k is the image lag (%) calculated by Eq. (1). The computation was repeated while L_k was greater than 0.1. Figure 4 shows the process of creating a target with image lag. Figure 5 shows targets with and without image lag created by this method. The digital phantom of the lung nodule was inserted into chest images of a patient during respiration obtained with the FPD system (Fig. 6). The path of the target was determined based on the distinguishing shadows of pulmonary vessels around the insert position. Figure 7 shows the trajectory of the shadows of pulmonary vessels in the lower right lung, which was measured manually by one medical physicist (R.T.) with clinical experience in diagnostic imaging. The measurements were performed three times and the average was adopted as the gold standard in evaluation of the accuracy in target tracking. The movement speed was simulated in two patterns, 10 mm/s and 20 mm/s, covering the range of lung tumor movement in normal breathing.

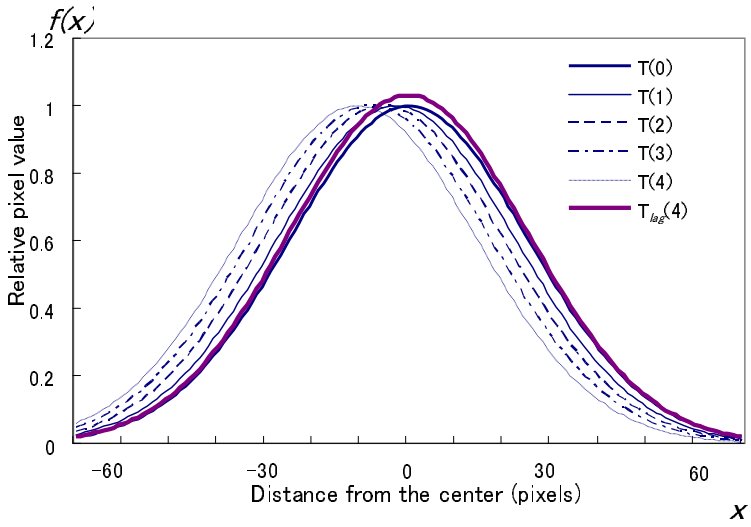

Figure 4. Process of creating a target with image lag, moving at a rate of 10 mm/s (X = 120, σ = 25, μ = 2.7 × k, 0 < k < 5). Half bandwidth of the distribution is given by 60 pixels. A round target 1 cm in diameter was created. The bold and solid lines show simulated target with image lag (n = 4), $T_{lag}(4)$.

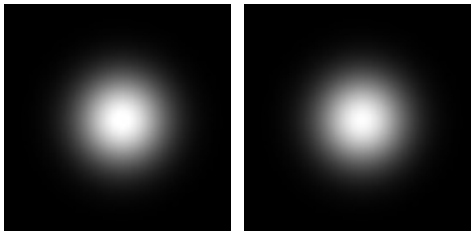

a | b

Figure 5. Simulated target (a) with and (b) without image lag (n = 4). The direction of movement is diagonally downward to the right.

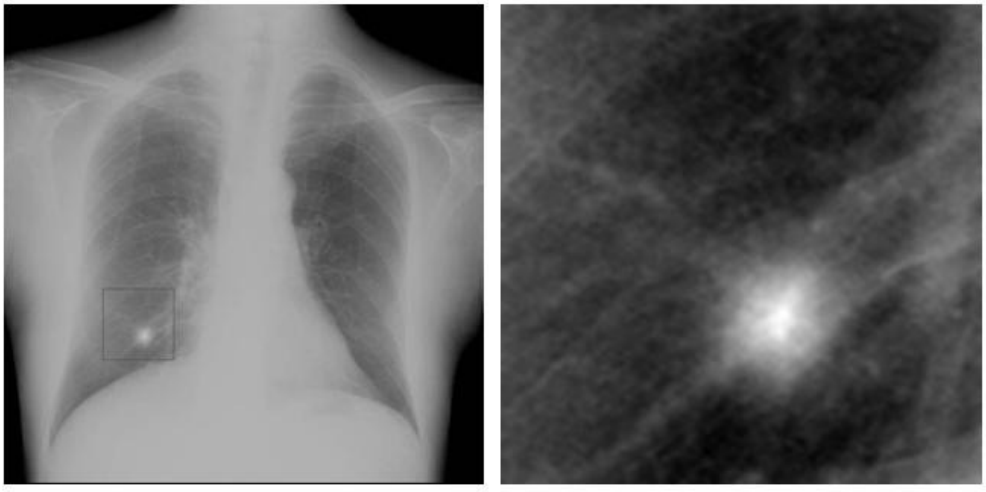

Figure 6. Simulated images with a lung tumor in the right lower lung (n=0).

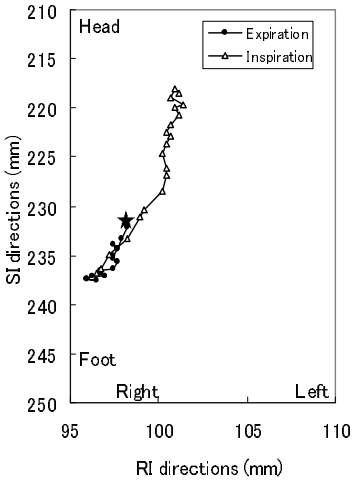

Figure 7. Trajectory of target determined based on the distinguishing shadows of pulmonary vessels around the inserted target on breathing chest radiographs. The path was given to simulated target. The star indicates frame # 0. (SI: Superior to Inferior, RL: Right to Left).

Trace of a moving target

The targets with and without image lag were tracked by a template-matching technique.[18] The summation of differences in pixel value (R) between the search area in the next frame, $S(x + dx, y + dy)$, and template in the current frame, $T(x, y)$, was expressed as follows:

$$R = \sum_{y=0}^{N} \sum_{x=0}^{M} \left| S(x+dx, y+dy) - T(x, y) \right| \tag{5}$$

$$(0 < x < M,\ 0 < y < N,\ -10 < dx < 10,\ -10 < dy < 10)$$

M and N are the size of the template, and dx and dy are the search range. The smallest R value was obtained when there were more similarities in the search area and template. The amount of shift (dx, dy) in the search area was determined by minimizing R, and the coordinates after movement were expressed as $(x + dx, y + dy)$. In this study, the initial template was given as a region to which the target was inserted in the first frame. After the second frame, a matching region of interest in the previous frame was used as the new template. The size of template was 100 × 100, search range was ± 10 pixels, and thus the search area was 120 × 120 pixels, determined based on the movement rate of the target. The targets moving at rates of 10 mm/s and 20 mm/s were displaced by 2.7 pixels/frame and 5.4 pixels/frame, respectively. The displacements were sufficiently covered by a search range of ± 10 pixels.

Data analysis

Four image sets with a moving target were assessed in the present study at 10 mm/s or 20 mm/s with and without image lag. The targets were tracked automatically and compared with the results of manual tracking. Tracking errors were calculated to evaluate the influence of blurring due to image lag on the accuracy of target tracking.

.

3. RESULTS

3.1 Image lag properties

Figure 8a shows the average pixel values measured in the ROIs. The average pixel values were reduced immediately after X-ray cutoff and reached the minimum value in the fifth ($n = 5$) frame after X-ray cutoff. Subsequently, they increased slightly and achieved a stable state at the end of the image sequence. Figure 8b shows image lag (L_n) for frame $n = 0$ through $n = 9$. The image lag for the first ($n = 1$), second ($n = 2$), third ($n = 3$), and fourth ($n = 4$) frames after X-ray cutoff were 2.0%, 0.85%, 0.37%, and 0.10%, respectively, and dropped to less than 0.10% in the fifth ($n = 5$) frame after X-ray cutoff.

MTF properties and edge profile curves

Figure 9 shows the profile curves obtained on the edges of a tungsten materials plate. From the profile, the edges were steep slopes composed of three to four pixels and the slopes of the moving plate were more gradual than those of the static plate. There was no visible difference between the falling and rising edges of the plate. There was also no significant difference in the profile curves at rates of 10 mm/s and 20 mm/s. Figure10 shows the MTF of a static tungsten materials plate and a plate moving at a rate of 10 mm/s. The results indicated that the present FPD system had good MTF properties. The MTF of a moving plate was much lower than that of a static plate; however, there was no significant difference between the falling and rising edges of the plate. Figure 11 shows the MTF measured on the falling edge of a static tungsten material plate and plates moving at rates of 10 mm/s and 20 mm/s. There were also no significant differences in MTF of a target moving at rates of 10 mm/s and 20 mm/s. The results obtained by measurement of edge profile curves were supported by the MTF measurements, as shown in Figs. 9 – 11.

Effects of image lag on target tracking

The target could be traced within a margin for error (± 5 mm) in external radiotherapy. Figure 12a shows the results regarding automatic tracking of a moving target with and without image lag at a rate of 10 mm/s. The maximum tracking errors of a target with and without image lag were 4.2 mm and 4.5 mm, respectively. Figure 12b shows the results in a target moving at a rate of 20 mm/s. The maximum errors in tracking target were 3.5 mm for both targets with and without image lag.

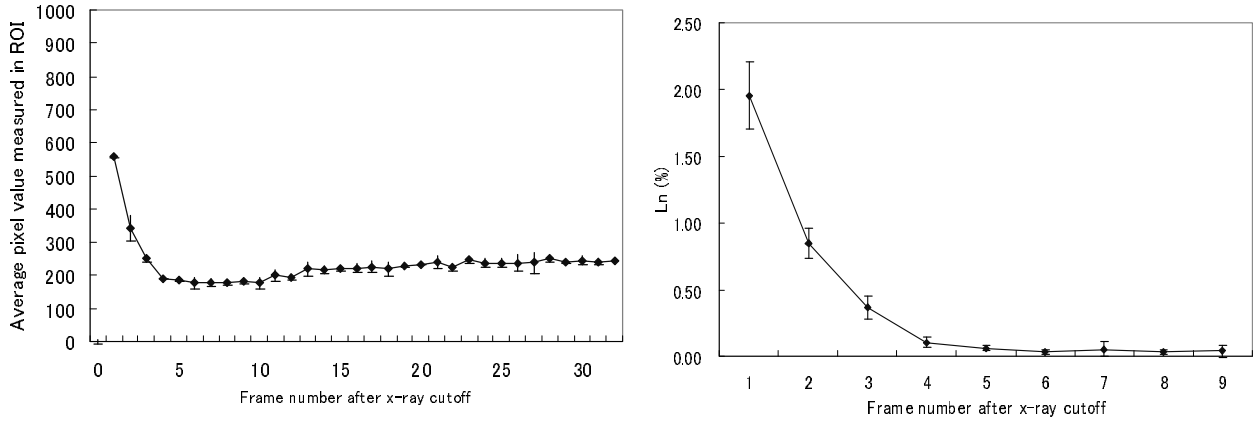

Figure 8. Image Lag properties. (a) Average pixel values measured in the ROIs. (b) L_n for frame n=0 through n=9. Error bars show ±SD.

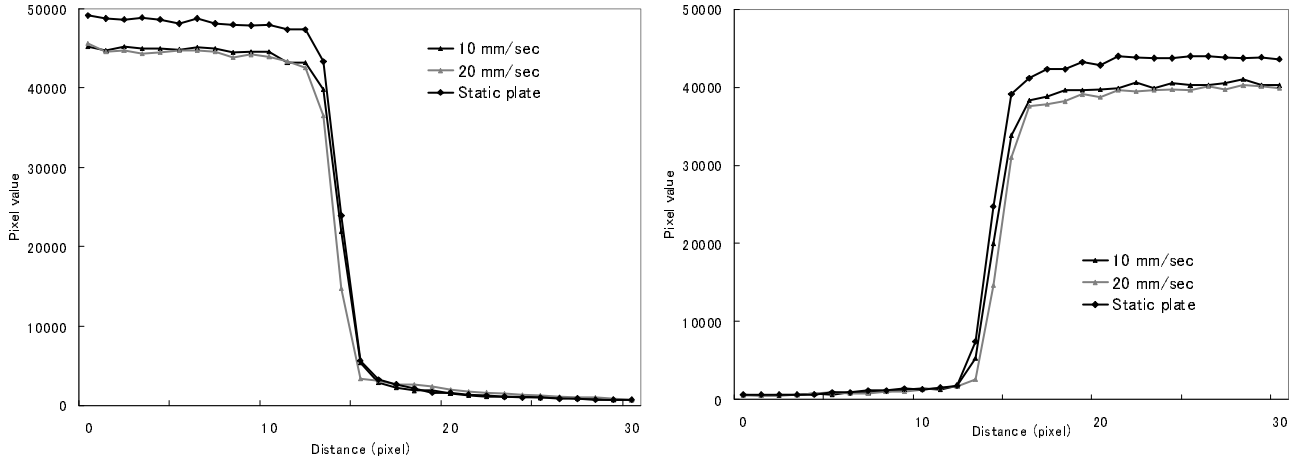

Figure 9. Profile curves obtained on (a) falling and (b) rising edges of a tungsten materials plate.

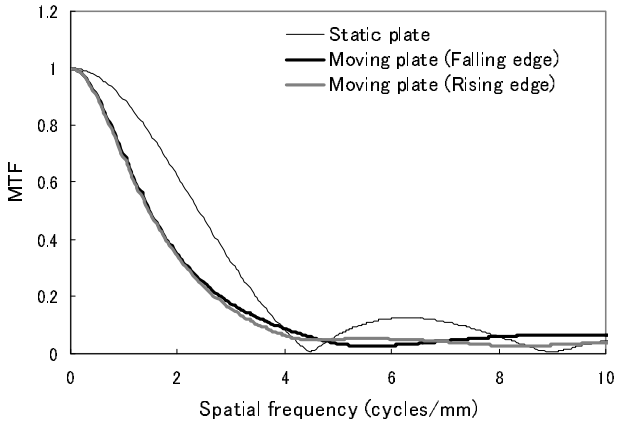

Figure 10. MTF of static and moving tungsten materials plate at a rate of 10 mm/s measured on a falling and rising edge.

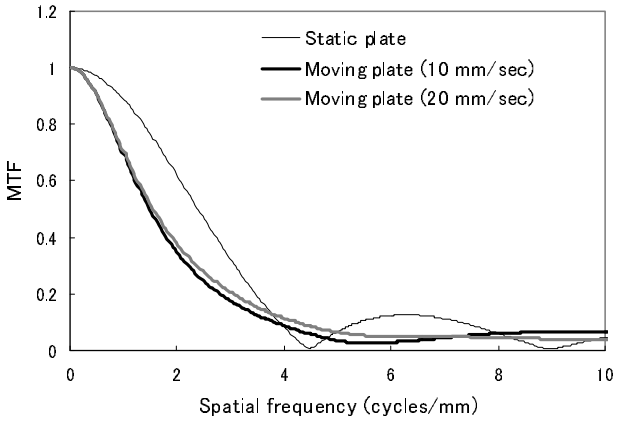

Figure 11. MTF of static and moving tungsten materials plate at a rate of 10 mm/s and 20 mm/s measured on a falling edge.

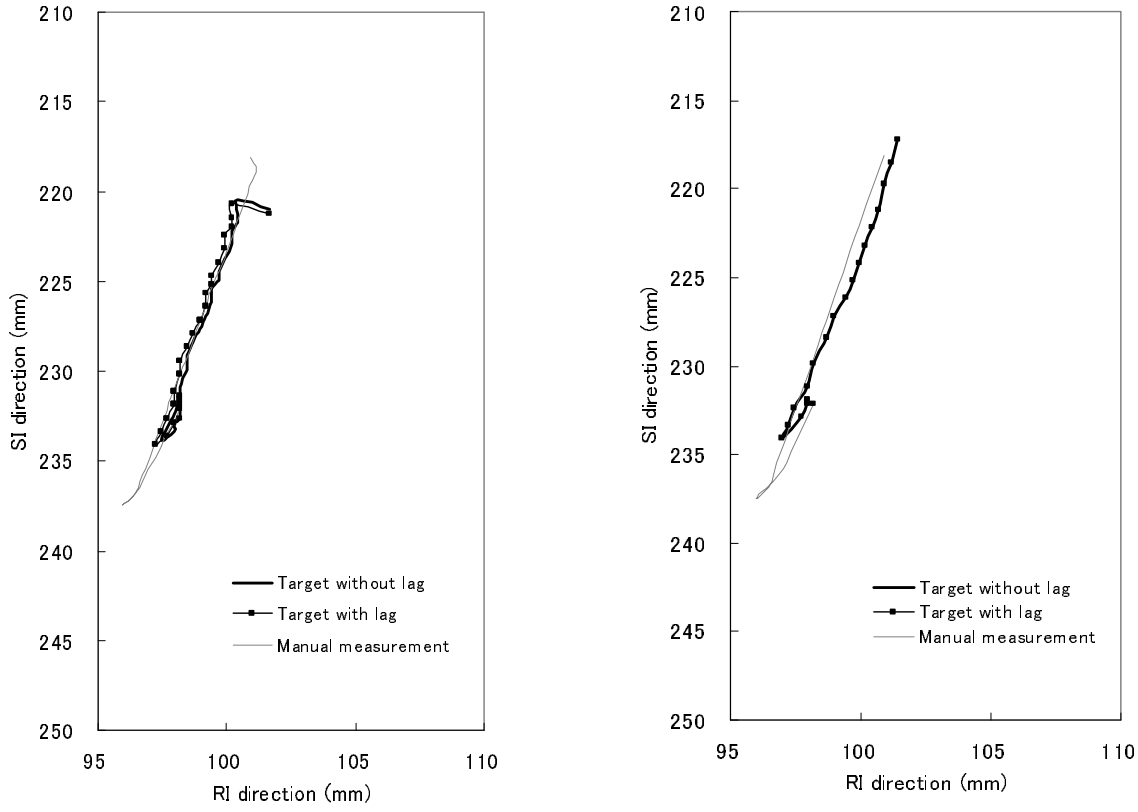

Figure 12. Automatic tracking of a moving target with and without image lag at a rate of (a) 10 mm/s and (b) 20 mm/s.

4. DISCUSSIONS

There are a number of factors that reduce the accuracy of target tracking in external radiation therapy. In terms of image quality, image lag, noise, contrast, and resolution are thought to reduce the accuracy of tracking. In the present study, we investigated image lag properties of a dynamic FPD system in target tracking for external radiotherapy. The image lag for the first frame (n = 1) after X-ray cutoff was 2.0% and decreased to less than 0.1% in the fifth frame in our direct type dynamic FPD system. These results were consistent with those reported by other groups.[10-12] In the measurement of profile curves on the edges of static and moving tungsten material plates, the effect of image lag was seen as blurred edges of the plate. In the MTF measurement, the blurred edges of a moving target were indicated as reduction of MTF. In the present study, there were no visible or significant differences in the profile curves and MTF between movement rates of 10 mm/s and 20 mm/s, or between falling and rising edges of a moving plate. The results suggested that there is no need to consider contour blurring due to image lag under normal breathing. However, to address the threshold of movement rate that impacts target tracking, further studies are required to investigate various movement rates and imaging conditions.

These lag properties, reduction of MTF and visible contour blurring of a moving target, increased concerns about the effects on target tracking in external radiotherapy, *i.e.*, out of track due to false detection of the target. In the simulation experiment, however, all motion targets created using such lag properties could be tracked within an error of ± 5 mm, which is an acceptable margin of error in external radiotherapy.[19] In addition, there were no significant differences in maximum error between targets with and without image lag. The results indicated that image lag had no effect on target tracking in external radiation therapy. This can be accountable for by the fact that there are only a few pixels of interframe movement of the target under normal conditions of quiet breathing during radiotherapy. The present results suggested that, factors other than image lag, such as image noise, contrast, and resolution, would have greater deleterious effects on tracking accuracy. However, it is possible that a simulated target created based on a Gaussian distribution originally has a bullring counter, and thus the effect of a bullring resulting from image lag was not actually evaluated. Further studies are also required to investigate the effect of target size and shape.

There was a problem in the results of tracking simulated images. Although the maximum errors were within the acceptable range, accuracy was not satisfactory. In addition, the maximum error was slightly larger in a target without than with lag. This was thought to be because motion of target was simulated based on trajectories of shadows around the inserted target. To give a constant movement rate to the target through all frames, such as 10 mm/s or 20mm/s, there may be some differences in the movement between a simulated target and the other shadows, including the template. Such conditions often result in tracking errors. In fact, a preliminary study showed that larger templates caused more errors. Thus, although outside the original purpose of this study, it was also shown to be important to optimize the size of the template and search area to improve the accuracy of target tracking.

In external radiation therapy, real-time tumor tracking has been achieved by diagnostic X-ray imaging with a dynamic FPD. Image quality has been improved markedly in comparison to megavoltage imaging. Although there is concern about added patient dose by fluoroscopic imaging to monitor motion target, higher image quality will result in more accurate target tracking. However, imaging should be performed with the minimum exposure dose to obtain images with the necessary accuracy of target tracking. Imaging parameters are dependent on the patient's body type and treatment area. Therefore, a simulation system would be very useful to determine appropriate imaging parameters in consideration of total patient dose. In the present study, we investigated image lag properties associated with target tracking in external radiotherapy, and showed that there was no effect of image lag on target tracking at usual breathing speed under conditions associated with radiotherapy. Further studies are required to investigate the influence of other factors, such as exposure dose, target size and shape, imaging rate, and thickness of the patient's body.

5. CONCLUSIONS

We investigated image lag propertis of a dynamic FPD system under conditions of target tracking in external radiotherapy. Image lag properties were assessed and a moving target with image lag was simulated using the results. The simulated target was tracked within a margin for error in external radiotherapy. In addition, there was no significant difference between the target with and without image lag. The results indicated that there was no effect of image lag on target tracking in external radiation therapy. Further studies are required to investigate the effect of a variety of parameters, such as target size, imaging rate, thickness of the patient's body, source to target distance, and exposure dose.

ACKNOWLEDGMENTS

This work was performed in the National Institute of Radiological Sciences (NIRS) in Japan. The authors are grateful to the staffs at Shimadzu Co., LTD, who assisted with data acquisition.

REFERENCES

1. Jaffray, D.A., Siewerdsen, J.H., Wong, J.W., Martinez, A.A., "Flat-panel cone-beam computed tomography for image-guided radiation therapy," Int J Radiat Oncol Biol Phys. 53, 1337-1349(2002)
2. Moore, C.J., Amer, A., Marchant, T., Sykes, J.R., Davies, J., Stratford, J., McCarthy, C., MacBain, C., Henry, A., Price P., Williams, P.C., "Developments in and experience of kilovoltage X-ray cone beam image-guided radiotherapy," Br J Radiol. 79, 66-78(2006)
3. Huntzinger, C., Munro, P., Johnson, S., Miettinen, M., Zankowski, C., Ahlstrom, G., Glettig, R., Filliberti, R., Kaissl, W., Kamber, M., Amstutz, M., Bouchet, L., Klebanov, D., Mostafavi, H., Stark, R., "Dynamic targeting image-guided radiotherapy," Med Dosim. 31, 113-125(2006)
4. Zhao, W., Degrescenzo, G., and Rowlands, J.A., "Investigation of lag and ghosting in amorphous selenium flat-panel detectors," Proc. SPIE 4682, 9-20 (2002).
5. Bloomquist, A.K., Yaffe, M.J., Mawdsley, G.E., Hunter, D.M., Beideck, D.J., "Lag and ghosting in a clinical flat-panel selenium digital mammography system," Med Phys. 33, 2998-3005(2006)
6. Siewerdsen, J. H. and Jaffray, D. A., "A ghost story: Spatio-temporal response characteristics of an indirect detection flat-panel imager," Med.Phys. 26, 1624-1641(1999)
7. Choquette, M., Rougeot, H., Martin, J., Laperriere, L., Shukri, Z., and Polischuk, B., "Direct selenium x-ray detector for fluoloscopy, R&F, and radiography," Proc. SPIE 3977, 128-136(2000)
8. Adachi, S, Hori, N., Sato, K., Tokuda, S., Sato, T., Uehara, K., Izumi, Y., Nagata, H., Yoshimura Y., and Yamada, S., "Experimental evaluation of a-Se and CdTe flat-panel detectors for digital radiography and fluoroscopy," Proc. SPIE 3977, 38-47(2000).
9. Schroeder, C., Stanescu, T., Rathee, S., Fallone, B.G., "Lag measurement in an a-Se active matrix flat-panel imager," Med Phys. 31, 1203-1209(2004)
10. Pokischuk, B., Shukri, Z., Legros, A., and Rougeot, H., "Selenium direct converter structure for static and dynamic x-ray detection in medical imaging applications," Proc. SPIE 3336, 494-504(1998)
11. Lee, D.L., Cheung, L.K., Rodricks, B., and Powell, G.F., "Improved imaging performance of 14x17-inch direct radiography system using Se/TFT detector," Proc. SPIE. 3336, 14-23(1998)
12. Tsukamoto, A., Yamada, S., Tomisaki, T., Tanaka, M., Sakaguchi, T., Asahina, H., Suzuki, K., Ikeda, M., "Development and evaluation of a large-area selenium-based flat panel detector for real-time radiography and fluoroscopy," Proc. SPIE 3659, 14-23 (1999)
13. Overdick, M., Solf, T. and Wischmann, H., "Temporal artifacts in flat dynamic x-ray detectors," Proc. SPIE 4320, 47-58(2001)
14. Friedman, S.N., and Cunningham, I.A., "A Method to measure the temporal MTF to determine the DQE of fluoroscopy system," Proc. SPIE 6142, 61421X-1-61421X-11 (2006) Friedman SN, Cunningham IA.
15. Friedman, S.N., and Cunningham, I.A., "A small-signal approach to temporal modulation transfer functions with exposure-rate dependence and its application to fluoroscopic detective quantum efficiency," Med Phys. 36, 3775-85(2009)
16. International electrotechnical commission, IEC International standard 62220-1, "Medical diagnostic X-ray equipment-Characteristics of digital imaging devices-Part 1: Determination of the detective quantum efficiency," Geneva, Switzerland(2003)
17. International electrotechnical commission, IEC International standard 62220-1, "Medical diagnostic X-ray equipment-Characteristics of digital imaging devices-Part 3: Characteristics of digital X-ray imaging devices-Part 1-3: Determination of the detective quantum efficiency – detectors used in dynamic imaging," Geneva, Switzerland(2008)
18. Ballard DH, Brown CM. Computer vision. Englewood Cliffs, New Jersey: Prentice-hall; 1982.
19. Kutcher, G.J., Goia, L., Gillin, M., Hanson, W.F., Leibel, S., Morton, R.J., Palta, J.R., Purdy, J.A., Reinstein, L.E., Svensson, G.K., et al. "Comprehensive QA for radiation oncology: Report of AAPM radiation therapy committee task group 40," Med Phys. 21, 581-618(1994)

REFERENCE LINKING

[1] Jaffray, D.A., Siewerdsen, J.H., Wong, J.W., Martinez, A.A., "Flat-panel cone-beam computed tomography for image-guided radiation therapy," Int J Radiat Oncol Biol Phys. 53, 1337-1349(2002)

[2] Moore, C.J., Amer, A., Marchant, T., Sykes, J.R., Davies, J., Stratford, J., McCarthy, C., MacBain, C., Henry, A., Price P., Williams, P.C., "Developments in and experience of kilovoltage X-ray cone beam image-guided radiotherapy," Br J Radiol. 79, 66-78(2006)

[3] Huntzinger, C., Munro, P., Johnson, S., Miettinen, M., Zankowski, C., Ahlstrom, G., Glettig, R., Filliberti, R., Kaissl, W., Kamber, M., Amstutz, M., Bouchet, L., Klebanov, D., Mostafavi, H., Stark, R., "Dynamic targeting image-guided radiotherapy," Med Dosim. 31, 113-125(2006)

[4] Zhao, W., Degrescenzo, G., and Rowlands, J.A., "Investigation of lag and ghosting in amorphous selenium flat-panel detectors," Proc. SPIE 4682, 9-20 (2002).

[5] Bloomquist, A.K., Yaffe, M.J., Mawdsley, G.E., Hunter, D.M., Beideck, D.J., "Lag and ghosting in a clinical flat-panel selenium digital mammography system," Med Phys. 33, 2998-3005(2006)

[6] Siewerdsen, J. H. and Jaffray, D. A., "A ghost story: Spatio-temporal response characteristics of an indirect detection flat-panel imager," Med.Phys. 26, 1624-1641(1999)

[7] Choquette, M., Rougeot, H., Martin, J., Laperriere, L., Shukri, Z., and Polischuk, B., "Direct selenium x-ray detector for fluoloscopy, R&F, and radiography," Proc. SPIE 3977, 128-136(2000)

[8] Adachi, S, Hori, N., Sato, K., Tokuda, S., Sato, T., Uehara, K., Izumi, Y., Nagata, H., Yoshimura Y., and Yamada, S., "Experimental evaluation of a-Se and CdTe flat-panel detectors for digital radiography and fluoroscopy," Proc. SPIE 3977, 38-47(2000).

[9] Schroeder, C., Stanescu, T., Rathee, S., Fallone, B.G., "Lag measurement in an a-Se active matrix flat-panel imager," Med Phys. 31, 1203-1209(2004)

[10] Pokischuk, B., Shukri, Z., Legros, A., and Rougeot, H., "Selenium direct converter structure for static and dynamic x-ray detection in medical imaging applications," Proc. SPIE 3336, 494-504(1998)

[11] Lee, D.L., Cheung, L.K., Rodricks, B., and Powell, G.F., "Improved imaging performance of 14x17-inch direct radiography system using Se/TFT detector," Proc. SPIE. 3336, 14-23(1998)

[12] Tsukamoto, A., Yamada, S., Tomisaki, T., Tanaka, M., Sakaguchi, T., Asahina, H., Suzuki, K., Ikeda, M., "Development and evaluation of a large-area selenium-based flat panel detector for real-time radiography and fluoroscopy," Proc. SPIE 3659, 14-23 (1999)

[13] Overdick, M., Solf, T. and Wischmann, H., "Temporal artifacts in flat dynamic x-ray detectors," Proc. SPIE 4320, 47-58(2001)

[14] Friedman, S.N., and Cunningham, I.A., "A Method to measure the temporal MTF to determine the DQE of fluoroscopy system," Proc. SPIE 6142, 61421X-1-61421X-11 (2006) Friedman SN, Cunningham IA.

[15] Friedman, S.N., and Cunningham, I.A., "A small-signal approach to temporal modulation transfer functions with exposure-rate dependence and its application to fluoroscopic detective quantum efficiency," Med Phys. 36, 3775-85(2009)

[16] International electrotechnical commission, IEC International standard 62220-1, "Medical diagnostic X-ray equipment-Characteristics of digital imaging devices-Part 1: Determination of the detective quantum efficiency," Geneva, Switzerland(2003)

[17] International electrotechnical commission, IEC International standard 62220-1, "Medical diagnostic X-ray equipment-Characteristics of digital imaging devices-Part 3: Characteristics of digital X-ray imaging devices-Part 1-3: Determination of the detective quantum efficiency – detectors used in dynamic imaging," Geneva, Switzerland(2008)

[18] Ballard DH, Brown CM. Computer vision. Englewood Cliffs, New Jersey: Prentice-hall; 1982.

[19] Kutcher, G.J., Goia, L., Gillin, M., Hanson, W.F., Leibel, S., Morton, R.J., Palta, J.R., Purdy, J.A., Reinstein, L.E., Svensson, G.K., et al. "Comprehensive QA for radiation oncology: Report of AAPM radiation therapy committee task group 40," Med Phys. 21, 581-618(1994)